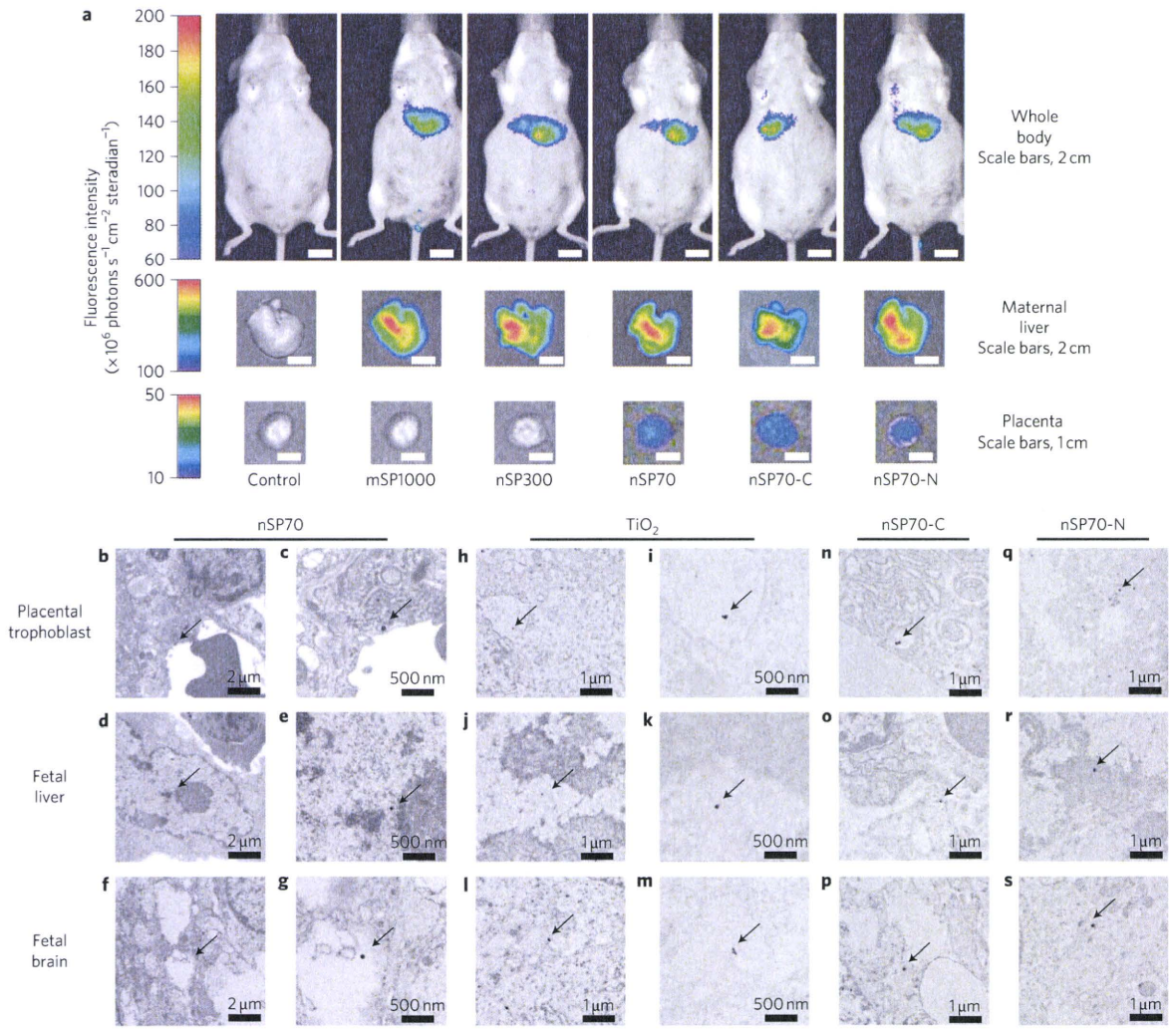

Figure 1 | Biodistribution of nanoparticles in pregnant mice. a, *In vivo* fluorescence images. Pregnant mice at GD16 were treated with 0.8 mg DY-676-labelled silica particles per mouse (nSP70, nSP300, mSP1000, nSP70-C or nSP70-N) or PBS (control), intravenously, through the tail vein. After 24 h, optical images of the whole body, maternal liver and placenta were acquired with a Xenogen IVIS 200 imaging system. **b–s**, TEM images of placentae and fetuses at GD18. Pregnant mice were treated intravenously with 0.8 mg per mouse of nSP70, nano-TiO_2, nSP70-C or nSP70-N on two consecutive days (GD16 and GD17). Arrows indicate nanoparticles. These particles were present in placental trophoblast cells (**b**,**c**,**h**,**i**,**n**,**q**), fetal liver cells (**d**,**e**,**j**,**k**,**o**,**r**) and fetal brain cells (**f**,**g**,**l**,**m**,**p**,**s**).

with nSP300 and mSP1000 did not show any significant abnormalities when compared to control mice (Fig 3b,d). Spiral artery canals failed to form (Fig. 3b,d) and blood flow was reduced in the fetal vascular sinuses of nSP70-treated mice (Fig. 3c,e). To further elucidate the influence of nanoparticles on placental dysfunction, we are examining the pathological histology of the placenta in nano-TiO_2-treated mice at present.

The areas including the placental major layers (the spongiotrophoblast and labyrinth) in nSP70-treated and control mice were examined by periodic acid–Schiff (PAS) staining (Fig. 3f–i). The total areas of placentae from each nSP70-treated mouse were not significantly different from those of control mice (Fig. 4a). The area of the spongiotrophoblast layer (Fig. 4b) and the ratio of the spongiotrophoblast layer area to the total placental area (Fig. 4c) in nSP70-treated mice were almost 50% smaller than those observed in control mice. The percentage of nuclei positively stained by terminal transferase-mediated dUTP nick end-labelling (TUNEL) was significantly higher within the spongiotrophoblast layer of nSP70-treated mice than within that of control mice, indicating that nSP70 induced apoptotic cell death of spongiotrophoblasts (Fig. 3j,k; Fig. 4d). The surrounding lengths of the villi in the labyrinth layer of nSP70-treated mice were significantly decreased compared to those of control mice (Fig. 3l,m; Fig. 4f), whereas the ratio of the labyrinth layer area to the total placental area in nSP70-treated mice was not significantly different from that of control mice (Fig. 4e). These results suggest that nSP70-induced pregnancy complications were probably caused by placental cellular damage, which might affect maternal–fetal exchange.

Normal placental development requires the coordinated expression of vascular endothelial growth factor (VEGF) and its receptor, fms-like tyrosine kinase-1 (Flt-1)[36]. Soluble Flt-1 (sFlt-1) is expressed by placental cells including spongiotrophoblasts, and is a potent anti-angiogenic molecule that regulates the generation of placental vasculature during pregnancy by sequestering circulating VEGF and regulating the action of VEGF[37]. The plasma level of sFlt-1 in nSP70- and nano-TiO_2-treated mice was significantly

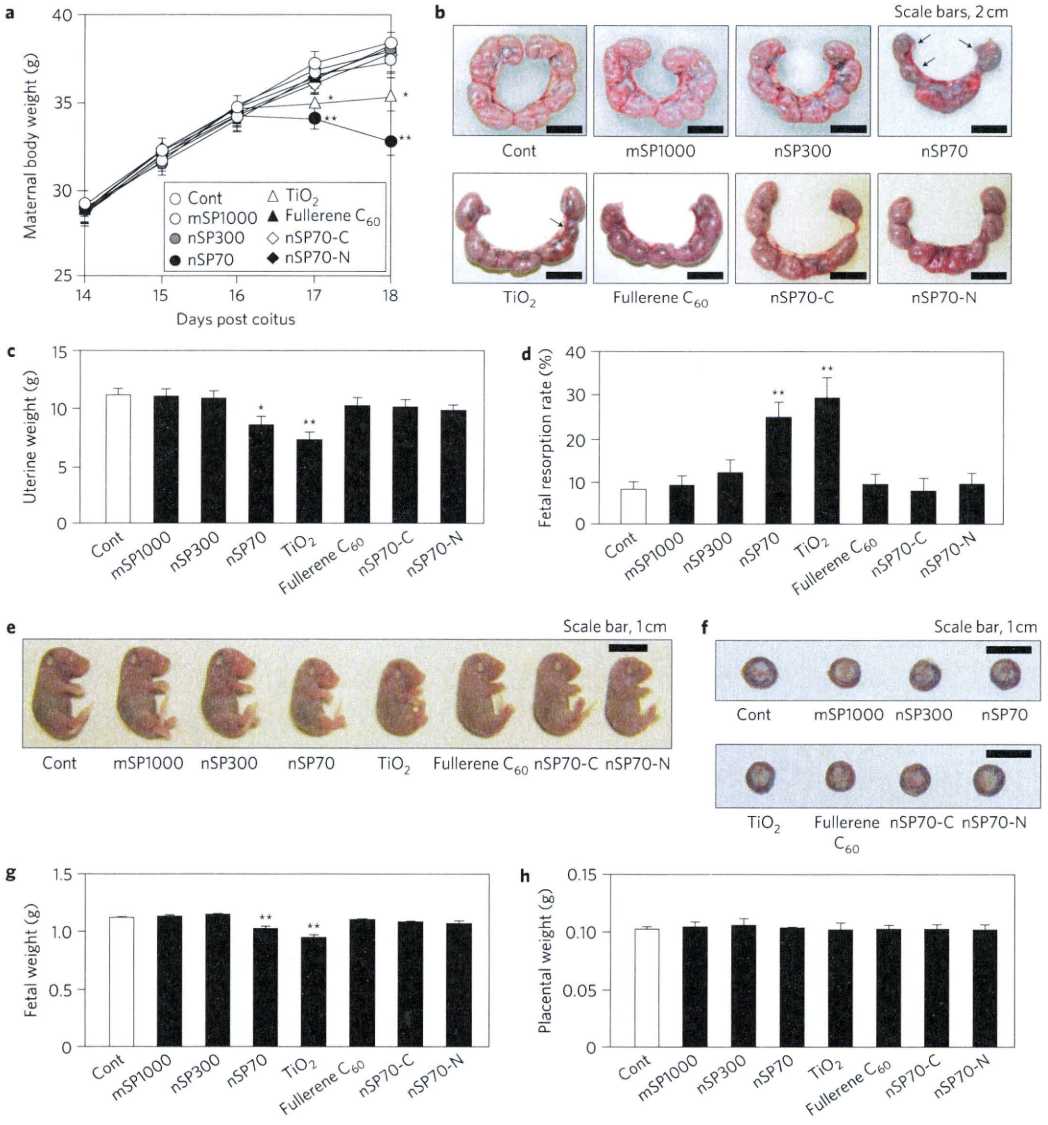

Figure 2 | Pregnancy complications in nSP70- or nano-TiO_2-treated mice. Pregnant mice were treated intravenously with 0.8 mg per mouse of nSP70, nSP300, mSP1000, nano-TiO_2, fullerene C_{60}, nSP70-C, nSP70-N or PBS (control) on two consecutive days (GD16 and GD17). **a**, Changes in maternal body weight. Maternal body weights were evaluated daily ($n = 11$–24). Statistically significant difference from control mice, $^*P < 0.05$ and $^{**}P < 0.01$ by ANOVA. **b**–**h**, Pregnancy complications. Uteri from mice were excised at GD18 (**b**). Uterine weights (**c**) and fetal resorption rates (**d**) were evaluated ($n = 11$–24). Fetuses (**e**) and placentae (**f**) were excised from uteri. Fetal weights (**g**) and placental weights (**h**) were evaluated ($n = 37$–212). All data represent means ± s.e.m ($^*P < 0.05$, $^{**}P < 0.01$ versus value for control mice by ANOVA).

lower than in control mice and those receiving nSP300, mSP1000, fullerene, nSP70-C and nSP70-N (Supplementary Fig. S7a–d), indicating that nSP70 induced not only structural abnormalities, but also functional abnormalities, in the mouse placenta.

The anticoagulation agent heparin is often administered to prevent miscarriage and IUGR[38]. Mice treated with a combination of nSP70 and heparin had slightly increased maternal body weights and decreased fetal resorption rates compared to mice that were not treated with heparin (Fig. 5a,c). Heparin treatment prevented decreases in uterine and fetal weight in nSP70-treated mice (Fig. 5b,d). Mice treated with a combination of nSP70 and heparin had similar levels of sFlt-1 to control mice (Supplementary Fig. S7e). These results suggest that the mechanism for nSP70-induced pregnancy complications might involve coagulation. However, it has recently been shown that heparin acts in many ways other than as an anticoagulant[39–42]. The anti-complement activation effect of heparin has been suggested to be important in mitigating pregnancy complications[40]. Complement activation induces neutrophil activation and this may lead to placental dysfunction, miscarriage, fetal growth restriction or pre-eclampsia[43,44]. Here, we have shown that the number of granulocytes in nSP70-treated mice is significantly higher than in control mice (Supplementary Fig. S5), indicating that nSP70 might have induced complement activation, which may have subsequently activated neutrophils and systemic inflammation.

Some reports have shown that heparin may also act as a placental growth factor, because heparin is known to inhibit placental apoptosis, stimulate placental proliferation and enhance the effect of several growth factors[39,41,42]. Moreover, oxidative stress in the placenta is known to cause placental dysfunction and to induce pregnancy

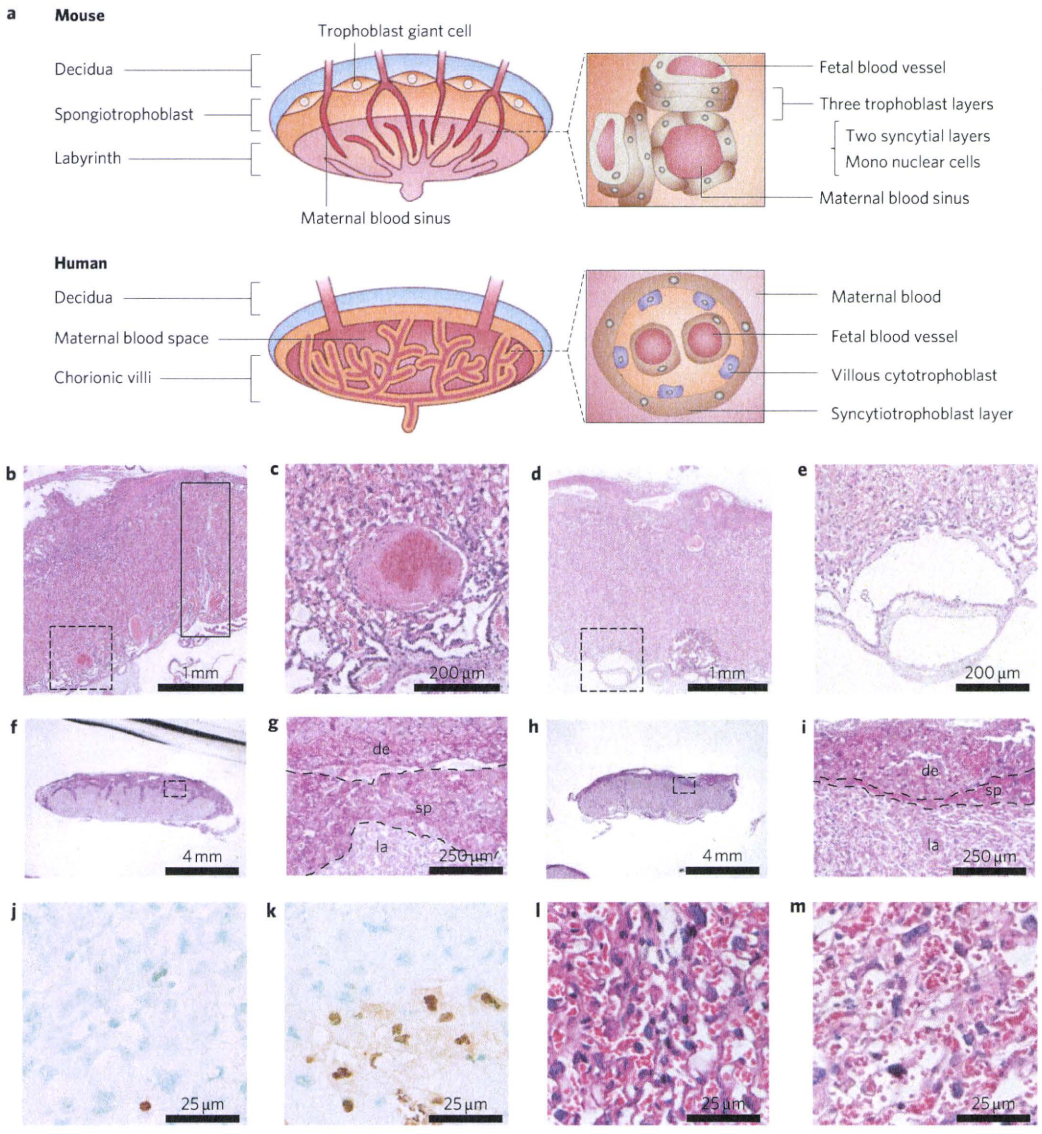

Figure 3 | Pathological examination of placenta. a, Schematic showing the differences between human and mouse placentae. **b–m**, Histological examination. Pregnant mice were treated intravenously with 0.8 mg per mouse of nSP70 or PBS (control) on two consecutive days (GD16 and GD17). At GD18, sections of placentae from PBS- (**b**,**c**,**f**,**g**) or nSP70-treated mice (**d**,**e**,**h**,**i**) were stained with H&E (**b–e**) or PAS (**f–i**). The solid box in **b** indicates the presence of spiral arteries and canals. Panels **c**, **e**, **g**, and **i** are enlarged images of the areas within the dashed boxes in **b**, **d**, **f** and **h**, respectively. In **g** and **i**, dashed lines delineate the decidua (de), spongiotrophoblast layer (sp) and labyrinth layer (la). Spongiotrophoblast layers of PBS- (**j**) or nSP70-treated mice (**k**) were stained with TUNEL. Labyrinth layers of PBS- (**l**) or nSP70-treated mice (**m**) were stained with H&E.

complications[45]. Nanomaterials have been reported to cause oxidative stress, which in turn induces cell apoptosis and inflammation[22,46,47]. Therefore, the pregnancy complications observed here might have been caused by oxidative stress induced by nSP70.

We have observed that the induction of oxidative stress in cells and the activation of the coagulation pathway in mice treated with nSP70-C and nSP70-N were lower than those observed in cells and mice treated with nSP70 (unpublished data). Therefore, we speculate that the lower activation of coagulation, complement and oxidative stress in the placenta of mice treated with nSP70-C and nSP70-N might have prevented pregnancy complications in those mice. It has recently been shown that nanomaterials become coated with serum proteins and induce different cellular responses by binding to proteins[48]. In addition, different surface characteristics, such as surface charge, are known to influence the binding affinities of proteins to nanomaterials[48]. Therefore, the differences in protein binding among nSP70, nSP70-C and nSP70-N might have given rise to differences in the fetotoxicity of the nanomaterials.

It should be noted that there are differences between mouse and human placentae, such as the greater role of yolk sac placentation in the mouse and the anatomy in the labyrinth[49,50] (Fig. 3a). The yolk sac plays a significant role in material transport from mother to fetus in mice, especially before the placental circulation is established[49]. Therefore, the accumulation of nSP70 in the yolk sac should be investigated to understand the accumulation mechanism of nanoparticles in fetuses. In the mouse placenta, three trophoblast layers embrace the fetal vasculature in the labyrinth layer, whereas in the human term placenta, a single syncytial layer with an underlying trophoblast stem cell layer is present in the villi[49,50]. As these anatomical and structural differences might affect nanoparticle

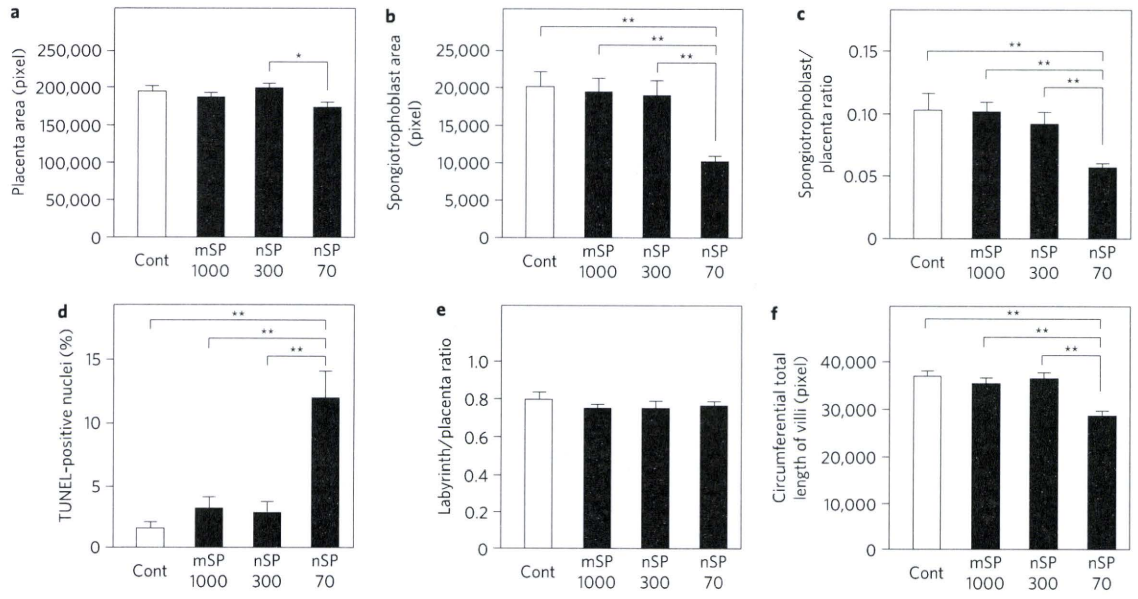

Figure 4 | Dysfunction of placentae. Pregnant mice were treated intravenously with 0.8 mg per mouse of nSP70, nSP300, mSP1000 or PBS (control) on two consecutive days (GD16 and GD17). **a**–**e**, At GD18, the area of the placenta (**a**) and the spongiotrophoblast layer (**b**) and the ratios of the spongiotrophoblast layer area to the total placental area (**c**) and of the labyrinth layer area to the total placental area (**e**) were assessed by examining the PAS-stained sections in Fig. 3f–i and were analysed quantitatively. The apoptotic index (**d**) was assessed by examining the TUNEL-stained sections in Fig. 3j,k and was quantitatively analysed. The surrounding length of the villi (**f**) in the labyrinth layers was assessed by examining the H&E-stained sections in Fig. 3l,m and was quantitatively analysed. All data represent means ± s.e.m. ($n = 11$–20; $^*P < 0.05$ and $^{**}P < 0.01$ by ANOVA).

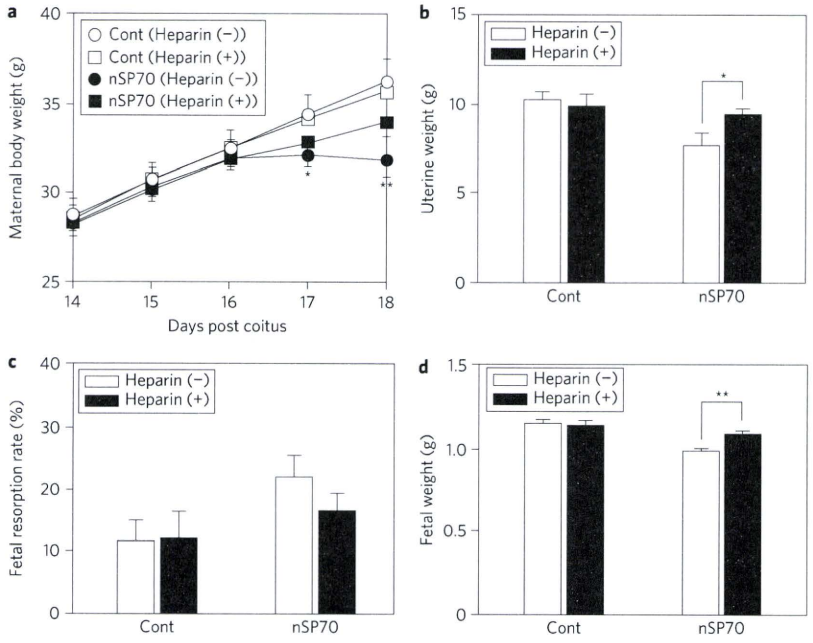

Figure 5 | Prevention of nSP70-induced pregnancy complications with heparin. Pregnant mice were treated intravenously with 0.8 mg per mouse of nSP70 or PBS (control) through the tail vein with or without heparin on two consecutive days (GD16 and GD17). **a**, Changes in maternal body weights. Maternal body weights were evaluated daily ($n = 10$–15). Statistically significant difference from control mice, $^*P < 0.05$ and $^{**}P < 0.01$ by ANOVA. **b**–**d**, Analysis of pregnancy complications in nSP70-treated mice with or without heparin treatment. At GD18, uterine weights (**b**), fetal resorption rates (**c**) and fetal weights (**d**) were evaluated (**b**,**c**, $n = 10$–15; **d**, $n = 55$–89). All data represent means ± s.e.m., $^*P < 0.05$ and $^{**}P < 0.01$ by Student's *t*-tests.

uptake and distribution, we cannot extrapolate our data about the placental distribution of nanoparticles, or placental dysfunction induced by nanoparticles, to humans. Additional studies that examine the penetration efficiency of nanoparticles into the human placenta (using *ex vivo* human placental tissue) are needed, as are studies that focus on the relationship between pregnancy complications and the amount of nanoparticles in the human placenta.

Conclusion

Of the materials studied here, nSP70 and nano-TiO_2 induced fetal resorption and restricted the growth of fetuses in pregnant mice, whereas fullerene C_{60} did not induce these complications. nSP70 and nano-TiO_2 were observed in the placenta, fetal liver and fetal brain, and nSP70 induced complications only at the highest concentration (0.8 mg per mouse) administered. The detrimental effects seen in nSP70-treated mice were linked to structural and functional changes in the placenta. Modification of the surface of nSP70 with carboxyl or amine groups abrogated the negative effects, suggesting the importance of surface charge. Although the nSP70 and nano-TiO_2 were mainly designed for experimental and industrial use, and not for cosmetics or food, we suggest that the potential fetotoxicity of these and other nanomaterials should be investigated more carefully.

Methods

Particles. nSP70, nSP300, mSP1000, nSP70-C and nSP70-N, as well as nSP70, nSP300 and mSP1000 labelled with DY-676 (excitation and emission wavelengths of 674 and 699 nm, respectively), were purchased from Micromod Partikeltechnologie. Rutile-type TiO_2 particles with a diameter of 35 nm (designated nano-TiO_2, Tayca Corporation) were also used. Polyvinylpyrrolidone (PVP)-wrapped fullerene C_{60} was provided by Vitamin C60 BioResearch Corporation. The nanoparticles were used after 5 min of sonication (280 W output (Ultrasonic Cleaner, AS One) and 1 min of vortexing.

Mice. Pregnant BALB/c mice (8–10 weeks) were purchased from Japan SLC. The experimental protocols conformed to the ethical guidelines of Osaka University and the National Institute of Biomedical Innovation, Japan.

***In vivo* imaging.** *In vivo* fluorescence imaging was performed with an IVIS 200 small-animal imaging system (Xenogen). At GD16, pregnant BALB/c mice were injected with 100 μl (0.8 mg per mouse) DY-676-labelled nSP70, nSP300, mSP1000, nSP70-C, nSP70-N or PBS (control), intravenously through the tail vein. At 24 h post-injection, the mice were anaesthetized, and images were obtained with a cy5.5 filter set (excitation/emission, 615–665 nm/695–770 nm). Imaging parameters were selected and implemented with Living Image 2.5 software (Xenogen).

TEM analysis. Pregnant BALB/c mice were treated with 100 μl (0.8 mg per mouse) of nSP70, nSP300, mSP1000, nSP70-C, nSP70-N or nano-TiO_2, intravenously through the tail vein, on two consecutive days (GD16 and GD17). At GD18, mice were killed after being anaesthetized, and the placenta, fetal liver and fetal brain were fixed in 2.5% glutaraldehyde for 2 h. Small pieces of tissue collected from these samples were washed with phosphate buffer, postfixed in sodium cacodylate-buffered 1.5% osmium tetroxide for 60 min at 4 °C, dehydrated using a series of ethanol concentrations, and embedded in Epon resin. The samples were examined under a Hitachi electron microscope (H-7650; Hitachi).

Fetotoxicity. Pregnant BALB/c mice were treated with 100 μl of nSP70 (0.2 mg, 0.4 mg or 0.8 mg per mouse), nSP300 (0.8 mg per mouse), mSP1000 (0.8 mg per mouse), nSP70-C (0.8 mg per mouse), nSP70-N (0.8 mg per mouse), nano-TiO_2 (0.8 mg per mouse), fullerene C_{60} (0.8 mg per mouse) or PBS (control), intravenously through the tail vein, on two consecutive days (GD16 and GD17). All mice were killed after being anaesthetized at GD18. Blood samples were collected in tubes containing 5 IU ml^{-1} heparin sodium, and plasma was harvested. The rate of fetal resorption was calculated (number of resorptions/total number of formed fetuses and resorptions). The fetuses and placentae of each mouse were excised and weighed, and the weight of the uterus calculated as the sum of the placental and fetal weights. To study the effects of heparin in nSP70-treated mice, pregnant BALB/c mice were treated with 100 μl (0.8 mg per mouse) nSP70 or PBS (control) intravenously through the tail vein on two consecutive days (GD16 and GD17). The same mice were treated with heparin (Sigma-Aldrich, 10 U) intraperitoneally on two consecutive days (GD16 and GD17), twice a day, 3 h before nSP70 treatment and 3 h after nSP70 treatment.

Histological examination. After fixing placentae in 10% formalin neutral buffer solution overnight, tissues were washed in PBS, dehydrated in a graded series of ethanol and xylene solutions, and embedded in paraffin. Sections (2 μm) were cut with a microtome. Sections were deparaffinized, rehydrated in a graded series of ethanols, and stained with H&E or PAS. Stained sections were dehydrated in a series of ethanols and mounted using permount. Representative histological images were recorded with a charge-coupled device (CCD) digital camera fixed to a microscope. The areas of the placenta, spongiotrophoblast layer and labyrinth layer were assessed by examining light microscopy images (Olympus) of the PAS-stained sections and were quantitatively analysed with Image J Imaging System Software Version 1.3 (National Institutes of Health). The circumferential total length of villi was assessed by examining light microscopy images of the H&E-stained sections and quantitatively analysed with Image J Imaging System Software Version 1.3. The presence of apoptotic cells in placental sections was analysed by TUNEL assay (Millipore). The tissue was counterstained with methyl green. Photographs of TUNEL (brown) and methyl green (light blue) staining were captured at three randomly selected fields in the spongiotrophoblast layer. TUNEL-positive nuclei (apoptotic nuclei) and methyl green-stained nuclei (total nuclei) were counted in the spongiotrophoblast layer. The apoptotic index in each section was calculated as the percentage of spongiotrophoblast nuclei stained TUNEL-positive divided by the total number of methyl green-stained nuclei found within the spongiotrophoblast layer.

Statistical analysis. All results are presented as means ± standard error of the mean (s.e.m.). Statistical significance in the differences was evaluated by Student's *t*-tests or Tukey's method after analysis of variance (ANOVA).

Received 23 September 2010; accepted 28 February 2011; published online 3 April 2011

References

1. Konstantatos, G. & Sargent, E. H. Nanostructured materials for photon detection. *Nature Nanotech.* **5,** 391–400 (2010).
2. Augustin, M. A. & Sanguansri, P. Nanostructured materials in the food industry. *Adv. Food. Nutr. Res.* **58,** 183–213 (2009).
3. Bowman, D. M., van Calster, G. & Friedrichs, S. Nanomaterials and regulation of cosmetics. *Nature Nanotech.* **5,** 92 (2010).
4. Petros, R. A. & DeSimone, J. M. Strategies in the design of nanoparticles for therapeutic applications. *Nature Rev. Drug Discov.* **9,** 615–627 (2010).
5. Martin, K. R. The chemistry of silica and its potential health benefits. *J. Nutr. Health Aging.* **11,** 94–97 (2007).
6. Knopp, D., Tang, D. & Niessner, R. Review: bioanalytical applications of biomolecule-functionalized nanometer-sized doped silica particles. *Anal. Chim. Acta.* **647,** 14–30 (2009).
7. Kagan, V. E., Bayir, H. & Shvedova, A. A. Nanomedicine and nanotoxicology: two sides of the same coin. *Nanomedicine* **1,** 313–316 (2005).
8. Nel, A., Xia, T., Madler, L. & Li, N. Toxic potential of materials at the nanolevel. *Science* **311,** 622–627 (2006).
9. Fadeel, B. & Garcia-Bennett, A. E. Better safe than sorry: understanding the toxicological properties of inorganic nanoparticles manufactured for biomedical applications. *Adv. Drug. Deliv. Rev.* **62,** 362–374 (2010).
10. Poland, C. A. *et al.* Carbon nanotubes introduced into the abdominal cavity of mice show asbestos-like pathogenicity in a pilot study. *Nature Nanotech.* **3,** 423–428 (2008).
11. Donaldson, K., Murphy, F. A., Duffin, R. & Poland, C. A. Asbestos, carbon nanotubes and the pleural mesothelium: a review of the hypothesis regarding the role of long fibre retention in the parietal pleura, inflammation and mesothelioma. *Part. Fibre Toxicol.* **7,** 5 (2010).
12. Nabeshi, H. *et al.* Systemic distribution, nuclear entry and cytotoxicity of amorphous nanosilica following topical application. *Biomaterials* **32,** 2713–2724 (2011).
13. Nabeshi, H. *et al.* Amorphous nanosilica induce endocytosis-dependent ROS generation and DNA damage in human keratinocytes. *Part. Fibre Toxicol.* **8,** 1 (2011).
14. Koren, G., Pastuszak, A. & Ito, S. Drugs in pregnancy. *N. Engl. J. Med.* **338,** 1128–1137 (1998).
15. Tardiff, R. G., Carson, M. L. & Ginevan, M. E. Updated weight of evidence for an association between adverse reproductive and developmental effects and exposure to disinfection by-products. *Regul. Toxicol. Pharmacol.* **45,** 185–205 (2006).
16. Wigle, D. T. *et al.* Epidemiologic evidence of relationships between reproductive and child health outcomes and environmental chemical contaminants. *J. Toxicol. Environ. Health. B. Crit. Rev.* **11,** 373–517 (2008).
17. Mills, J. L. *et al.* Incidence of spontaneous abortion among normal women and insulin-dependent diabetic women whose pregnancies were identified within 21 days of conception. *N. Engl. J. Med.* **319,** 1617–1623 (1988).
18. Cetin, I. & Alvino, G. Intrauterine growth restriction: implications for placental metabolism and transport. A review. *Placenta* **30(Suppl. A),** S77–S82 (2009).
19. Godfrey, K. M. & Barker, D. J. Fetal nutrition and adult disease. *Am. J. Clin. Nutr.* **71,** 1344S–1352S (2000).
20. Barker, D. J. Adult consequences of fetal growth restriction. *Clin. Obstet. Gynecol.* **49,** 270–283 (2006).
21. Takeda, K. *et al.* Nanoparticles transferred from pregnant mice to their offspring can damage the genital and cranial nerve systems. *J. Health Sci.* **55,** 95–102 (2009).
22. Shimizu, M. *et al.* Maternal exposure to nanoparticulate titanium dioxide during the prenatal period alters gene expression related to brain development in the mouse. *Part. Fibre Toxicol.* **6,** 20 (2009).
23. Tian, F. *et al.* Surface modification and size dependence in particle translocation during early embryonic development. *Inhal. Toxicol.* **21(Suppl. 1),** 92–96 (2009).
24. Saunders, M. Transplacental transport of nanomaterials. *Wiley Interdiscip. Rev. Nanomed. Nanobiotechnol.* **1,** 671–684 (2009).

25. Chu, M. *et al.* Transfer of quantum dots from pregnant mice to pups across the placental barrier. *Small* **6,** 670–678 (2010).
26. Hougaard, K. S. *et al.* Effects of prenatal exposure to surface-coated nanosized titanium dioxide (UV-Titan). A study in mice. *Part. Fibre Toxicol.* **7,** 16 (2010).
27. He, X. *et al. In vivo* study of biodistribution and urinary excretion of surface-modified silica nanoparticles. *Anal. Chem.* **80,** 9597–9603 (2008).
28. Wick, P. *et al.* Barrier capacity of human placenta for nanosized materials. *Environ. Health Perspect.* **118,** 432–436 (2010).
29. Watson, R. E., Desesso, J. M., Hurtt, M. E. & Cappon, G. D. Postnatal growth and morphological development of the brain: a species comparison. *Birth Defects Res. B. Dev. Reprod. Toxicol.* **77,** 471–484 (2006).
30. Li, L. *et al. In vivo* delivery of silica nanorattle encapsulated docetaxel for liver cancer therapy with low toxicity and high efficacy. *ACS Nano.* **4,** 6874–6882 (2010).
31. Filipe, P. *et al.* Stratum corneum is an effective barrier to TiO_2 and ZnO nanoparticle percutaneous absorption. *Skin Pharmacol. Physiol.* **22,** 266–275 (2009).
32. Sadrieh, N. *et al.* Lack of significant dermal penetration of titanium dioxide from sunscreen formulations containing nano- and submicron-size TiO_2 particles. *Toxicol. Sci.* **115,** 156–166 (2010).
33. Albrecht, C. *et al.* Inflammatory time course after quartz instillation: role of tumor necrosis factor-alpha and particle surface. *Am. J. Respir. Cell. Mol. Biol.* **31,** 292–301 (2004).
34. Kibschull, M., Gellhaus, A. & Winterhager, E. Analogous and unique functions of connexins in mouse and human placental development. *Placenta* **29,** 848–854 (2008).
35. Gasperowicz, M. & Otto, F. The notch signalling pathway in the development of the mouse placenta. *Placenta* **29,** 651–659 (2008).
36. Lam, C., Lim, K. H. & Karumanchi, S. A. Circulating angiogenic factors in the pathogenesis and prediction of preeclampsia. *Hypertension* **46,** 1077–1085 (2005).
37. Hirashima, M., Lu, Y., Byers, L. & Rossant, J. Trophoblast expression of fms-like tyrosine kinase 1 is not required for the establishment of the maternal–fetal interface in the mouse placenta. *Proc. Natl Acad. Sci. USA* **100,** 15637–15642 (2003).
38. Derksen, R. H., Khamashta, M. A. & Branch, D. W. Management of the obstetric antiphospholipid syndrome. *Arthritis Rheum.* **50,** 1028–1039 (2004).
39. Li, Y., Wang, H. Y. & Cho, C. H. Association of heparin with basic fibroblast growth factor, epidermal growth factor, and constitutive nitric oxide synthase on healing of gastric ulcer in rats. *J. Pharmacol. Exp. Ther.* **290,** 789–796 (1999).
40. Girardi, G., Redecha, P. & Salmon, J. E. Heparin prevents antiphospholipid antibody-induced fetal loss by inhibiting complement activation. *Nature Med.* **10,** 1222–1226 (2004).
41. Hills, F. A. *et al.* Heparin prevents programmed cell death in human trophoblast. *Mol. Hum. Reprod.* **12,** 237–243 (2006).
42. Hossain, N., Schatz, F. & Paidas, M. J. Heparin and maternal fetal interface: why should it work to prevent pregnancy complications? *Thromb. Res.* **124,** 653–655 (2009).
43. Girardi, G., Yarilin, D., Thurman, J. M., Holers, V. M. & Salmon, J. E. Complement activation induces dysregulation of angiogenic factors and causes fetal rejection and growth restriction. *J. Exp. Med.* **203,** 2165–2175 (2006).
44. Redecha, P., van Rooijen, N., Torry, D. & Girardi, G. Pravastatin prevents miscarriages in mice: role of tissue factor in placental and fetal injury. *Blood* **113,** 4101–4109 (2009).
45. Myatt, L. & Cui, X. Oxidative stress in the placenta. *Histochem. Cell. Biol.* **122,** 369–382 (2004).
46. Hussain, S. *et al.* Oxidative stress and proinflammatory effects of carbon black and titanium dioxide nanoparticles: role of particle surface area and internalized amount. *Toxicology* **260,** 142–149 (2009).
47. Liu, X. & Sun, J. Endothelial cells dysfunction induced by silica nanoparticles through oxidative stress via JNK/P53 and NF-κB pathways. *Biomaterials* **31,** 8198–8209 (2010).
48. Lundqvist, M. *et al.* Nanoparticle size and surface properties determine the protein corona with possible implications for biological impacts. *Proc. Natl Acad. Sci. USA* **105,** 14265–14270 (2008).
49. Enders, A. C. & Blankenship, T. N. Comparative placental structure. *Adv. Drug Deliv. Rev.* **38,** 3–15 (1999).
50. Rossant, J. & Cross, J. C. Placental development: lessons from mouse mutants. *Nature Rev. Genet.* **2,** 538–548 (2001).

Acknowledgements

This study was supported in part by Grants-in-Aid for Scientific Research from the Ministry of Education, Culture, Sports, Science and Technology of Japan (MEXT) and from the Japan Society for the Promotion of Science (JSPS) through a Knowledge Cluster Initiative (MEXT). It was also supported by Health Labour Sciences Research Grants from the Ministry of Health, Labour and Welfare of Japan (MHLW), by a Global Environment Research Fund from the Minister of the Environment, and by the Food Safety Commission (Cabinet Office), the Cosmetology Research Foundation, the Smoking Research Foundation and the Takeda Science Foundation.

Author contributions

K.Y. and Y.Y. designed the study. K.Y., K.H., K.M., Y. Morishita, M.N., T. Yoshida, T.O., H.N., K.N., Y.A., H.K., Y. Monobe and T.I. performed the experiments. K.Y. and Y.Y. collected and analysed the data. K.Y. and Y.Y. wrote the manuscript. H.A., K.S., Y.K., T.M., S.T., N.I., I.Y., S.S. and T. Yoshikawa provided technical support and conceptual advice. Y.T. supervised the project. All authors discussed the results and commented on the manuscript.

Additional information

The authors declare no competing financial interests. Supplementary information accompanies this paper at www.nature.com/naturenanotechnology. Reprints and permission information is available online at http://npg.nature.com/reprintsandpermissions/. Correspondence and requests for materials should be addressed to Y.Y. and Y.T.

Laboratory of Bio-Functional Molecular Chemistry[1], Laboratory of Toxicology[2], Graduate School of Pharmaceutical Sciences, Osaka University, Osaka, Japan

Effect of 70-nm silica particles on the toxicity of acetaminophen, tetracycline, trazodone, and 5-aminosalicylic acid in mice

X. Li[1], M. Kondoh[1], A. Watari[1], T. Hasezaki[1], K. Isoda[1], Y. Tsutsumi[2], K. Yagi[1]

Received September 13, 2010, accepted October 15, 2010

Masuo Kondoh, Ph. D., Laboratory of Bio-Functional Molecular Chemistry
masuo@phs.osaka-u.ac.jp
Kiyohito Yagi, Ph. D., Laboratory of Bio-Functional Molecular Chemistry, Graduate School of Pharmaceutical Sciences, Osaka University, Suita, Osaka 565-0871, Japan
yagi@phs.osaka-u.ac.jp

Pharmazie 66: 1–5 (2011) *doi: 10.1691/ph.2011.0778*

Exposure to nano-sized particles is increasing because they are used in a wide variety of industrial products, cosmetics, and pharmaceuticals. Some animal studies indicate that such nanomaterials may have some toxicity, but their synergistic actions on the adverse effects of drugs are not well understood. In this study, we investigated whether 70-nm silica particles (nSP70), which are widely used in cosmetics and drug delivery, affect the toxicity of a drug for inflammatory bowel disease (5-aminosalicylic acid), an antibiotic drug (tetracycline), an antidepressant drug (trazodone), and an antipyretic drug (acetaminophen) in mice. Co-administration of nSP70 with trazodone did not increase a biochemical marker of liver injury. In contrast, co-administration increased the hepatotoxicity of the other drugs. Co-administration of nSP70 and tetracycline was lethal. These findings indicate that evaluation of synergistic adverse effects is important for the application of nano-sized materials.

1. Introduction

Nano-sized particles, which have a diameter of less than 100 nm, are widely used in medicine, food, and machinery. With their smaller size, the physical and chemical properties of their constituents change, so that they may be toxic, for example to the lungs or liver, even though macro-particles of the same materials are not (Byrne and Baugh 2008; Nishimori et al. 2009b). Some nano-sized particles show long-term accumulation or a wide distribution in the body (Byrne and Baugh 2008; Nishimori et al. 2009b; Xie et al. 2009; Yang et al. 2008).

Recent reports indicate that some nano-sized particles can generate reactive oxygen species (ROS) on their surfaces, leading to cellular injury (Jin et al., 2008; Sharma et al. 2007; Ye et al. 2010). There are also many drugs that cause adverse effects through the generation of ROS (Ali et al. 2002; Kovacic 2005; Xu et al. 2008). Thus, nano-sized particles might enhance the side-effects of some pharmaceutical drugs. Indeed, we have shown that 70-nm silica particles (nSP70) cause liver injury but that macro-sized silica particles with a diameter of 300 and 1000 nm do not (Nishimori et al. 2009b). Also, when co-administered to mice, nSP70 but not the macro-sized silica particles enhance the toxicity of cisplatin and paraquat (Nishimori et al. 2009a). Surprisingly, co-administration of cisplatin and nSP70 was lethal, suggesting that each chemical may have different synergistic effects in the presence of nano-sized materials. In the current study, to clarify the influence of nano-sized materials on the adverse effects of chemicals, we assessed the toxicity in mice of 5-aminosalicylic acid (an agent for treating inflammatory bowel disease), tetracycline (a broad-spectrum antibiotic), trazodone (an antidepressant), and acetaminophen (a common antipyretic analogue) in the presence or absence of nSP70.

2. Investigations and results

Several reports indicate that 5-aminosalicylic acid, which is used to treat inflammatory bowel disease, causes liver injury and interstitial nephritis (Deltenre et al. 1999; Margetts et al. 2001). Administration of 5-aminosalicylic acid caused an increase in ALT, AST and BUN levels (Fig. 1). Also, nSP70 dose-dependently elevated ALT and AST levels. Co-treatment with 5-aminosalicylic acid and nSP70 resulted in higher levels of ALT and AST than nSP70 alone. In contrast, changes in BUN levels in response to 5-aminosalicylic acid were not affected by nSP70.

Next, we investigated effect of nSP70 on tetracycline, a broad-spectrum antibiotic. As shown in Fig. 2A and 2B, administration of tetracycline did not elevate biochemical markers for liver injury. In contrast, co-administration with nSP70 resulted in the synergistic induction of liver injury. However, nSP70 alone did not cause kidney injury. Importantly, co-administration of 30 and 50 mg/kg nSP70 with tetracycline resulted in the death of 1 of 4 and 2 of 4 mice, respectively.

Finally, we investigated effect of nSP70 on toxicity of the antidepressant trazodone and the antipyretic analgesic acetaminophen. We found that nSP70 did not have a synergistic effect on the toxicity of trazodone (Fig. 3). In contrast, co-administration of acetaminophen with nSP70 caused synergistic liver injury (Fig. 4).

3. Discussion

In this study, we showed that nSP70 synergistically enhances the toxicity of 5-aminosalicylic acid, tetracycline, and acetaminophen but not trazodone. To avoid direct interac-

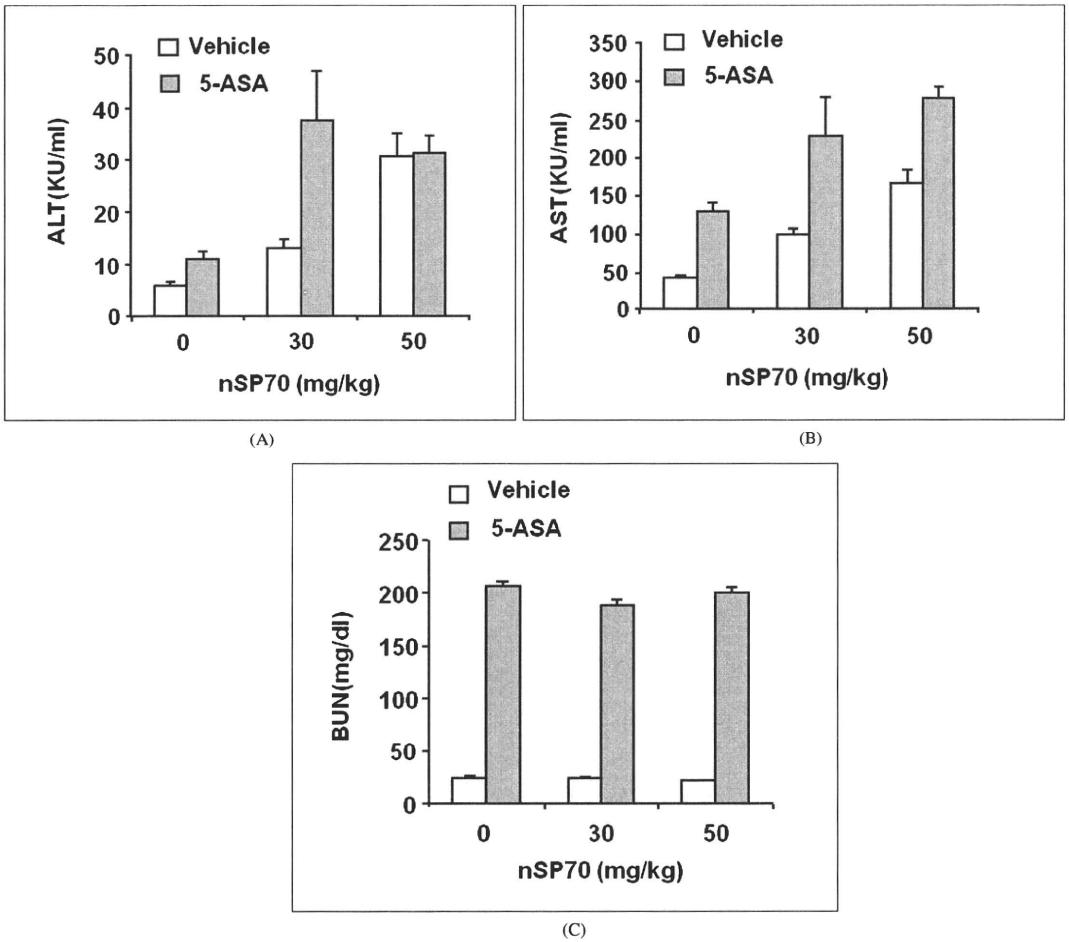

Fig. 1: Effect of nSP70 on 5-aminosalicylic acid (5-ASA)-induced toxicity Mice were injected intraperitoneally with 5-ASA at 0 (open column) or 500 mg/kg (gray column) and intravenously with nSP70 at the indicated doses. After 24 h, the serum was collected. Shown are the levels of ALT (A), AST (B), and BUN (C). Data are means ± SEM (n = 4)

tions between nSP70 and chemicals in their administration and absorption, nSP70 and chemicals were administered intravenously and intraperitoneally, respectively. Administration of nSP70 alone has been shown to cause liver injury but not kidney injury (Nishimori et al. 2009b). Also, in this study, nSP70 did not enhance kidney injury induced by 5-aminosalicylic acid or tetracycline, two drugs known to be nephrotoxic (Grisham et al. 1992; Kunin 1971). The renal toxicity of cisplatin, another nephrotoxic chemical, was unaffected by nSP70 (Nishimori et al. 2009a). Like 5-aminosalicylic acid, tetracycline, and acetaminophen (Chun et al. 2009; Herzog and Leuschner 1995; Kunin 1971), nSP70 is hepatotoxic (Nishimori et al. 2009b), and we showed here that its co-administration synergistically enhanced liver injury. These findings indicate that nSP70 may enhance the toxicity of certain chemicals. Therefore, it will be important to assess the tissue-specific risk of nano-sized materials.

The nSP70 particles had a lethal effect when combined with tetracycline. The 50% lethal dose of tetracycline is 318 mg/kg by intraperitoneal injection in mice. A previous report showed that 100 mg/kg nSP70 is lethal in 100% of mice (Nishimori et al. 2009b). A single injection of tetracycline (100 mg/kg) or nSP70 (30 or 50 mg/kg) alone was not lethal in this study but a combination of the two was. Co-administration of cisplatin and nSP70 showed a similar synergistic lethal effect. This could be due to an interaction between nSP70 and serum albumin. Tetracycline in the bloodstream can bind to albumin (Popov et al. 1972; Powis 1974). Likewise, serum albumin adsorbs onto nano-sized silica particles (Dutta et al. 2007). When injected intravenously, 100-nm anionized albumin-modified liposomes are taken up by hepatic endothelial cells and Kupffer cells (Kamps et al. 1997), which normally clear chemically modified albumin (Jansen et al. 1991). Thus, tetracycline-bound serum albumin may adsorb onto nSP70, causing it to be taken up by the hepatic endothelial cells and Kupffer cells in the liver where it may accumulate and cause lethal liver damage.

Indirect interactions between chemicals and nano-sized particles mediated by serum albumin may be useful for estimating the toxicity of nano-sized materials. In this study, co-treatment of mice with nSP70 (50 mg/kg) and tetracycline decreased BUN levels compared to tetracycline alone or nSP70 (30 mg/kg) and tetracycline. A similar decrease in BUN levels

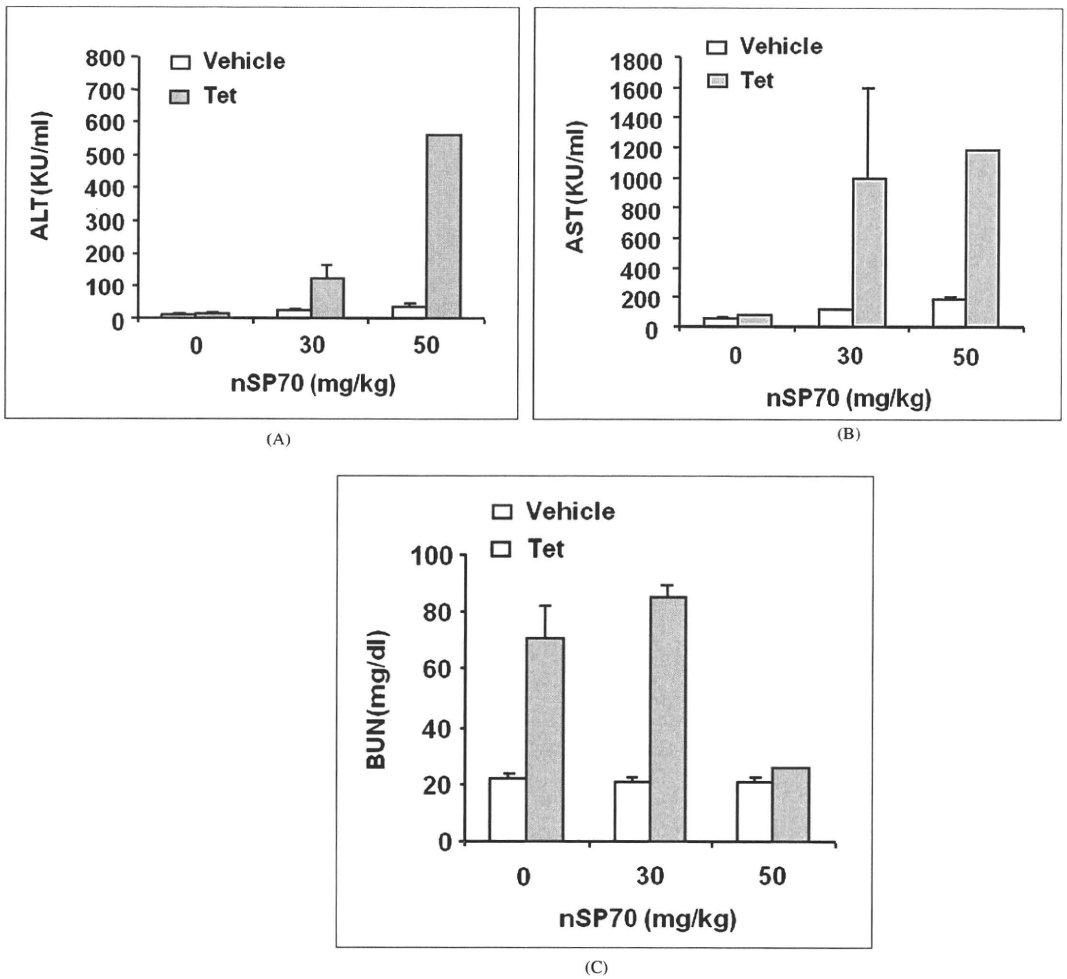

Fig. 2: Effect of nSP70 on tetracycline (Tet)-induced toxicity Mice were injected intraperitoneally with Tet at 0 (open column) or 100 mg/kg (gray column) and intravenously with nSP70 at the indicated doses. After 24 h, the serum was collected. Shown are the levels of ALT (A), AST (B), and BUN (C). One of 4 mice died when co-treated with nSP70 (30 mg/kg) and Tet (100 mg/kg), and 2 of 4 mice died when co-treated with nSP70 (50 mg/kg) and Tet (100 mg/kg). Data are means or means ± SEM (n = 2–4)

was also reported in mice co-treated with nSP70 and cisplatin (Nishimori et al. 2009a). However, the mechanism by which these decrease the BUN level remains to be determined.

In conclusion, we found that nSP70 causes synergistic toxicity when combined with some clinically used drugs, although the synergistic effects differ between chemicals. One combination was lethal, and the others resulted in tissue injury. These studies suggest that evaluation of possible synergistic adverse effects with pharmaceutical drugs may be important for assessing the safety of nano-sized particles.

4. Experimental

4.1. Materials

The nSP70 nanoparticles were obtained from Micromod Partikeltechnologie GmnH (Rostock, Germany). The mean diameter of the particles, as analyzed by a Zetasizer (Sysmex Co., Kobe, Japan), was 55.7 nm, and the particles were spherical and nonporous. The particles were stored at 25 mg/ml as an aqueous suspension. The suspensions were thoroughly dispersed by sonication before use and diluted in water. An equal volume of solution was injected for each treatment. Acetaminophen, tetracycline, and trazodone were dissolved in saline solution, and 5-aminosalicylic acid was suspended in 1% sodium salt of carboxy methyl cellulose. All reagents were of research grade.

4.2. Animals

Eight-week-old BALB/c male mice were purchased from Shimizu Laboratory Supplies Co., Ltd. (Kyoto, Japan). Mice were maintained in controlled environment (23 ± 1.5 °C; 12-h light/12-h dark cycle) with free access to standard rodent chow and water. The mice were given 1 week to adapt before experiments. All of the experimental protocols complied with the ethical guidelines of the Graduate School of Pharmaceutical Sciences, Osaka University.

4.3. Biochemical analysis

Serum alanine aminotransferase (ALT), aspartate aminotransferase (AST), and blood urea nitrogen (BUN) were measured using commercially available kits according to the manufacturer's protocols (WAKO Pure Chemical, Osaka, Japan).

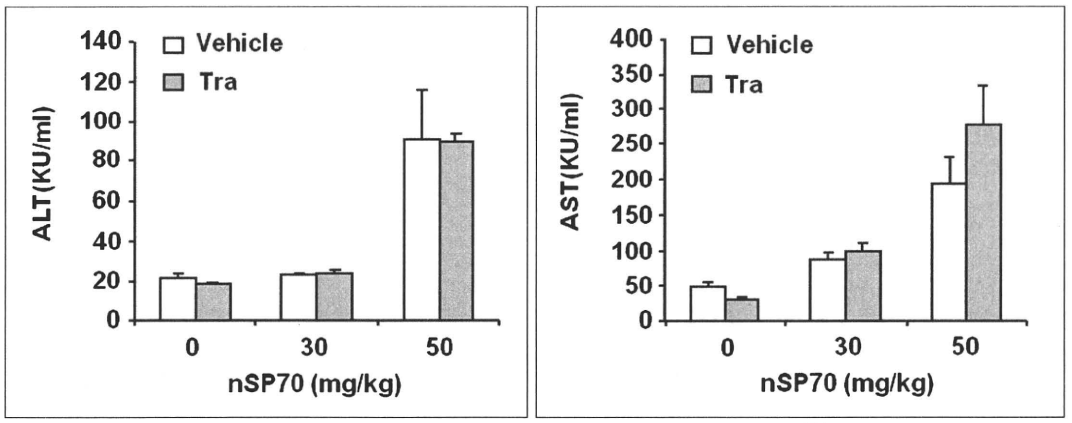

(A) (B)

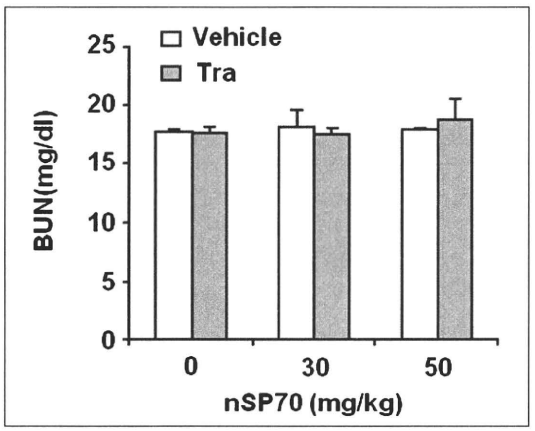

(C)

Fig. 3: Effect of nSP70 on trazodone (Tra)-induced toxicity Mice were injected intraperitoneally with Tra at 0 (open column) or 100 mg/kg (gray column) and intravenously with nSP70 at 30 or 50 mg/kg. After 24 h, the serum was collected. Shown are the levels of ALT (A), AST (B), and BUN (C). Data are means ± SEM (n = 4)

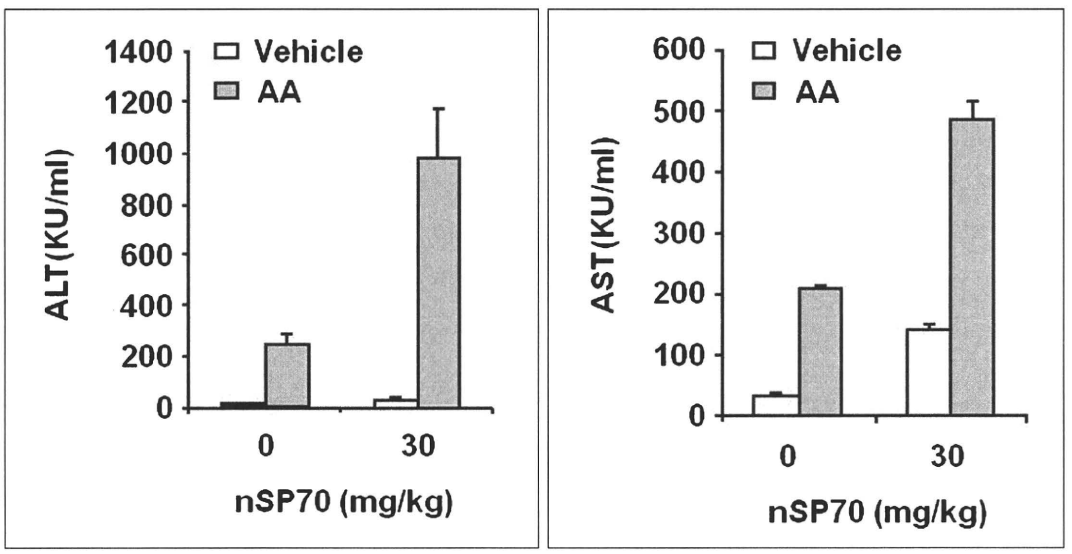

(A) (B)

Fig. 4: Effect of nSP70 on acetaminophen (AA)-induced toxicity Mice were injected intraperitoneally with AA at 0 (open column) or 500 mg/kg (gray column) and intravenously with nSP70 (30 mg/kg). After 24 h, the serum was collected. Shown are the levels of ALT (A) and AST (B). Data are means ± SEM (n = 4)

Acknowledgements: The authors thank all members of our laboratory for their useful comments and discussion. This study was supported by a grant from the Ministry of Health, Labor, and Welfare of Japan.

References

Ali MM, Frei E, Straub J, Breuer A Wiessler M (2002) Induction of metallothionein by zinc protects from daunorubicin toxicity in rats. Toxicology 179: 85–93.

Byrne JD Baugh JA (2008) The significance of nanoparticles in particle-induced pulmonary fibrosis. Mcgill J Med 11: 43–50.

Chun LJ, Tong MJ, Busuttil RW Hiatt JR (2009) Acetaminophen hepatotoxicity and acute liver failure. J Clin Gastroenterol 43: 342–349.

Deltenre P, Berson A, Marcellin P, Degott C, Biour M Pessayre D (1999) Mesalazine (5-aminosalicylic acid) induced chronic hepatitis. Gut 44: 886–888.

Dutta D, Sundaram SK, Teeguarden JG, Riley BJ, Fifield LS, Jacobs JM, Addleman SR, Kaysen GA, Moudgil BM Weber TJ (2007) Adsorbed proteins influence the biological activity and molecular targeting of nanomaterials. Toxicol Sci 100: 303–315.

Grisham MB, Ware K, Marshall S, Yamada T Sandhu IS (1992) Prooxidant properties of 5-aminosalicylic acid. Possible mechanism for its adverse side effects. Dig Dis Sci 37: 1383–1389.

Herzog R Leuschner J (1995) Experimental studies on the pharmacokinetics and toxicity of 5-aminosalicylic acid-O-sulfate following local and systemic application. Arzneimittelforschung 45: 300–303.

Jansen RW, Molema G, Harms G, Kruijt JK, van Berkel TJ, Hardonk MJ Meijer DK (1991) Formaldehyde treated albumin contains monomeric and polymeric forms that are differently cleared by endothelial and Kupffer cells of the liver: evidence for scavenger receptor heterogeneity. Biochem Biophys Res Commun 180: 23–32.

Jin CY, Zhu BS, Wang XF Lu QH (2008) Cytotoxicity of titanium dioxide nanoparticles in mouse fibroblast cells. Chem Res Toxicol 21: 1871–1877.

Kamps JA, Morselt HW, Swart PJ, Meijer DK Scherphof GL (1997) Massive targeting of liposomes, surface-modified with anionized albumins, to hepatic endothelial cells. Proc Natl Acad Sci U S A 94: 11681–11685.

Kovacic P (2005) Role of oxidative metabolites of cocaine in toxicity and addiction: oxidative stress and electron transfer. Med Hypotheses 64: 350–356.

Kunin CM (1971) Hepatorenal toxicity of tetracycline. Minn Med 5: 532–533.

Margetts PJ, Churchill DN Alexopoulou I (2001) Interstitial nephritis in patients with inflammatory bowel disease treated with mesalamine. J Clin Gastroenterol 32: 176–178.

Nishimori H, Kondoh M, Isoda K, Tsunoda S, Tsutsumi Y Yagi K (2009a) Influence of 70 nm silica particles in mice with cisplatin or paraquat-induced toxicity. Pharmazie 64 : 395–397.

Nishimori H, Kondoh M, Isoda K, Tsunoda S, Tsutsumi Y Yagi K (2009b) Silica nanoparticles as hepatotoxicants. Eur J Pharm Biopharm 72: 496–501.

Popov PG, Vaptzarova KI, Kossekova GP Nikolov TK (1972) Fluorometric study of tetracycline-bovine serum albumin interaction. The tetracyclines-a new class of fluorescent probes. Biochem Pharmacol 21: 2363–2372.

Powis G (1974) A study of the interaction of tetracycline with human serum lipoproteins and albumin. J Pharm Pharmacol 26: 113–118.

Sharma CS, Sarkar S, Periyakaruppan A, Barr J, Wise K, Thomas R, Wilson BL Ramesh GT (2007) Single-walled carbon nanotubes induces oxidative stress in rat lung epithelial cells. J Nanosci Nanotechnol 7: 2466–2472.

Xie G, Sun J, Zhong G, Shi L Zhang D (2009) Biodistribution and toxicity of intravenously administered silica nanoparticles in mice. Arch Toxicol, in press.

Xu JJ, Henstock PV, Dunn MC, Smith AR, Chabot JR de Graaf D (2008) Cellular imaging predictions of clinical drug-induced liver injury. Toxicol Sci 105: 97–105.

Yang ST, Wang X, Jia G, Gu Y, Wang T, Nie H, Ge C, Wang H Liu Y (2008) Long-term accumulation and low toxicity of single-walled carbon nanotubes in intravenously exposed mice. Toxicol Lett 181: 182–189.

Ye Y, Liu J, Xu J, Sun L, Chen M Lan M (2010) Nano-SiO2 induces apoptosis via activation of p53 and Bax mediated by oxidative stress in human hepatic cell line. Toxicol *In Vitro* 24: 751–758.

Laboratory of Bio-Functional Molecular Chemistry[1], Laboratory of Toxicology and Safety Science[2], Graduate School of Pharmaceutical Sciences[3], Osaka University, Suita; Laboratory of Biopharmaceutical Research (Pharmaceutical Proteomics), National Institute of Biomedical Innovation, Ibaraki, Osaka, Japan

Effect of surface charge on nano-sized silica particles-induced liver injury

K. ISODA[1], T. HASEZAKI[1], M. KONDOH[1], Y. TSUTSUMI[2,3], K. YAGI[1]

Received October 5, 2010, accepted November 11, 2010

Dr Kiyohito Yagi, Laboratory of Bio-Functional Molecular Chemistry, Graduate School of Pharmaceutical Sciences, Osaka University, Suita, Osaka 565-0871, Japan
yagi@phs.osaka-u.ac.jp

Pharmazie 66: 1–4 (2011) *doi: 10.1691/ph.2011.0808*

Nanomaterials are used frequently in microelectronics, cosmetics and sunscreen, and research for the development of nanomaterial-based drug delivery systems is promising. We previously reported that the intravenous administration of unmodified silica particles with a diameter of 70 nm (SP70) caused hepatic injury. Here, we examined the acute hepatic toxicity of SP70 modified with amino group (SP70-N) or carboxyl group (SP70-C). When administered intravenously into mice, SP70-N and SP70-C dose-dependently increased the serum level of alanine aminotransferase (ALT). However, the toxicity levels of surface charge-modified silica particles were much less weaker than the level of unmodified particles. When SP70 was repeatedly administered at 40 mg/kg twice a week for 4 weeks into mice, the hydroxyproline content of the liver significantly increased. Azan staining of the liver section indicated the extensive fibrosis. To the contrary, the repeated administration of SP70-N or SP70-C at 60 mg/kg twice a week for 4 weeks into mice did not cause the hepatic fibrosis. These findings suggest that the surface charge of nanomaterials could change their toxicity.

1. Introduction

Recently, the scientific, medical, and technical applications of nanomaterials have greatly increased. Nanomaterials are frequently used in microelectronics, cosmetics and sunscreen, and their potential use in drug-delivery systems is being investigated (Dobson 2006). Nanomaterials have unique physicochemical qualities as compared to micromaterials in regard to size, surface structure, solubility, and aggregation. Thus, the reduction in particle size from the micro- to nanoscale is beneficial for many industrial and scientific applications. However, nanomaterials have potential toxicity that is not found in micromaterials, and it is, therefore, essential to understand the biological activity and potential toxicity of nanomaterials (Warheit et al. 2008).

The physical properties of nanomaterials are changed by the modification of their surface charge, which extends their possible applications. For example, charge-modified dendrimers are expected to have applications in drug-delivery systems. The physical properties and the toxicity of carbon nanotubes change based on the surface charge (Smith et al. 2009), as do the pharmacokinetics of liposomes. Future research will undoubtedly lead to expanded applications of surface-modified nanomaterials, however, little has been reported on their toxicity.

Silica nanoparticles have been applied to diagnostic measures and drug delivery methods. Intraperitoneal administration of silica nanoparticles results in the biodistribution of the nanoparticles to diverse organs, such as the liver, kidney, spleen and lung (Kim et al., 2006). We previously found that nano-size silica particles with a diameter of 70 nm caused liver injury, while micro-size particles with a diameter of 300 or 1000 nm did not (Nishimori et al. 2009a, b). In the present study, we examined the hepatic toxicity of surface charge-modified silica nanoparticles.

2. Investigations, results and discussion

The surface modification technology has been developed in the field of nanotechnology (Schiestel et al. 2004), and many nanomaterials with new functions will be produced for cosmetics and medicinal use. Thus, it should be important to investigate the effect of surface charge of nanomaterials on living body.

We initially examined the acute toxicity of 70-nm diameter silica nanoparticles (SP70) modified with amino group (SP70-N) or carboxyl group (SP70-C) at the maximal dose of 100 mg/kg. Intravenous injection of 50 mg/kg of unmodified SP70 was lethal in mice (Fig. 1A). The acute liver toxicity of SP70-N and SP70-C increased in a dose-dependent manner (Fig. 1B, C). Intravenous injection of SP70-C was lethal in all mice at 100 mg/kg and was often lethal at 80 and 60 mg/kg. SP70-C was more toxic than SP70-N. We examined the hepatic injury caused by 40 mg/kg of unmodified SP70 and 60 mg/kg of modified SP70 (SP70-C and SP70-N). The hematoxylin-eosin staining of liver tissue from mice injected with the silica nanoparticles is shown in Fig. 2A–D. The liver injury caused by SP70 was more extensive than that caused by SP70-C and SP70-N. Significant increase in the levels of BUN, a biochemical marker of kidney injury, was not observed in mice that received the nanoparticles (Fig. 3). The less amount of unmodified SP70 induced significant liver damage than the surface-modified silica particles. Thus, the

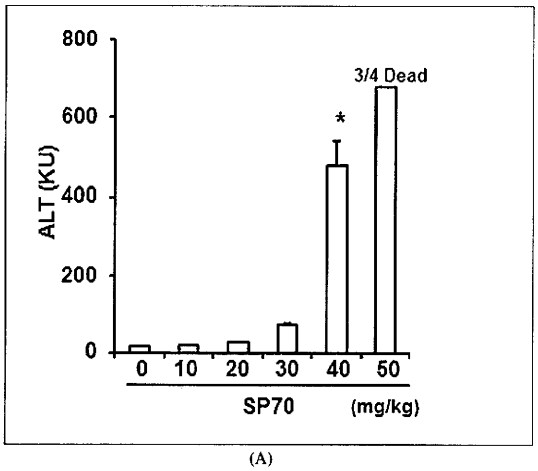

(A)

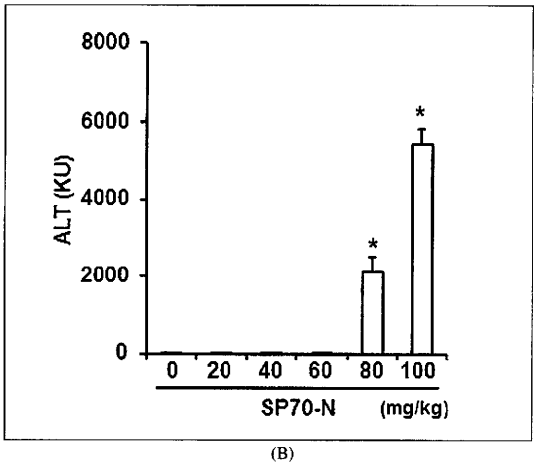

(B)

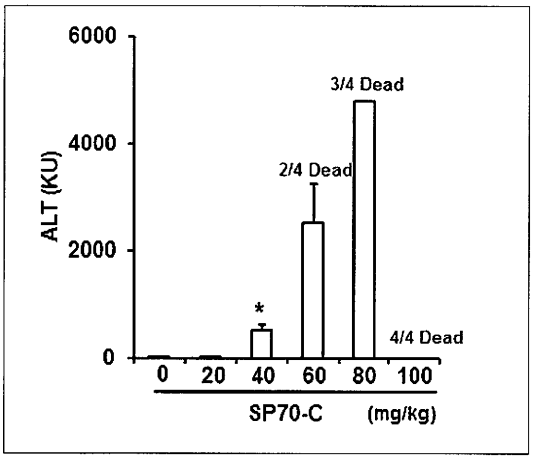

(C)

Fig. 1: Acute liver toxicity of SP70-N and SP70-C. SP70 (A), SP70-N (B) and SP70-C (C) were intravenously administered at the indicated doses. At 24 h after administration, blood was collected, and the resultant serum was used for the ALT assay. Serum BUN (H) at 24 h was measured using a commercially available kit. Data are means ± SEM (n = 4). *$p < 0.05$ as compared to the vehicle-treated group.

modification of the surface charge decreased the amount of acute hepatic injury caused by silica nanoparticles.

We then examined the chronic liver injury caused by 60 mg/kg of SP70-C or SP70-N as compared to 30 mg/kg of SP70. Nanoparticles were intravenously injected into mice twice a week for 4 weeks. We assessed the presence of liver fibrosis, because it is a symptom of chronic liver injury. We determined the hepatic hydroxyproline contents in the silica nanoparticle–treated mice (Fig. 4A). SP70, but not SP70-N or SP70-C, significantly increased the hepatic hydroxyproline content by 3.5-fold over the control value. Moreover, collagen, which accumulates in the fibrotic liver, was stained with Azan reagent, and blue-stained regions were observed in SP70-treated, but not SP70-C- and SP70-N-treated, liver sections (Fig. 4B-E). Thus, the chronic administration of SP70-C and SP70-N did not cause hepatic fibrosis in mice.

In this study we found that the surface modification of nanosilica particles with amino group and carboxyl group attenuated liver toxicity. We suspect that this decreased toxicity is due to a decrease in the amount of silica nanoparticles that accumulate in the liver. Oku et al. (1996) reported that the accumulation of liposomes in the liver changed depending on the surface charge of liposomes. Although we confirmed the presence of SP70-N, SP70-C and SP70 in the electron micrograph (data not shown), we were unable to compare the accumulative amounts in the liver. Therefore, an analysis of the accumulative amount of the silica nanoparticles in the liver is necessary in future studies.

The surface charge of nanoparticles might change the pharmacokinetics *in vivo*; for instance, the silica nanoparticles with a positive surface charge have increased paracellular permeability (Lin et al. 2007). Moreover, the phagocytosis of liposomes by hepatic Kupffer cells was promoted by a positive surface charge (Schiestel et al. 2004). We previously reported that the inhibition of phagocytosis by Kupffer cells increased the toxicity of nanosilica particles (Nishimori et al. 2009a). Therefore, it is thought that the nanoparticles with a positive surface charge have decreased hepatic toxicity due to increased phagocytosis by liver Kupffer cells.

This report is the first to indicate that altering the surface charge of nanomaterials changes their toxicity. Further studies based on these data will provide useful information regarding the safety of the nanomaterials.

3. Experimental

3.1. Materials

Silica particles with a diameter of 70 nm were obtained from Micromod Partikeltechnologie GmbH (Rostock, Germany). Silica particles with a diameter of 70 nm that were modified with the amino group or the carboxyl group were obtained from Micromod Partikeltechnologie GmbH (Rostock, Germany). The size distribution of the particles was analyzed using a Zetasizer (Sysmex Co., Kobe, Japan), and the mean diameters were 61.5 and 70.5 nm, respectively. The electric charge of the particles, also measured using the Zetasizer, was found to be −19.7 and −52.4 mV, respectively. The particles were spherical and nonporous and were stored at 25 mg/mL in an aqueous suspension. The suspensions were thoroughly dispersed by sonication before use and then diluted in ultrapure water. All reagents used were of research grade.

3.2. Animals

Eight-week-old BALB/c male mice were purchased from Shimizu Laboratory Supplies Co., Ltd. (Kyoto, Japan) and were maintained in a controlled environment (23 ± 1.5 °C; 12-h light/dark cycle) with access to standard rodent chow and water *ad libitum*. The mice were left to adapt to the new environment for 1 week before commencing with the experiment. Mice that received a single treatment of silica nanoparticles were anesthetized for sacrificing 24 h after intravenous injection. Mice in the frequent treatment group received intravenous administration of silica nanoparticles twice a week for 4 weeks. The experimental protocols conformed to the ethical guidelines of the Graduate School of Pharmaceutical Sciences, Osaka University.

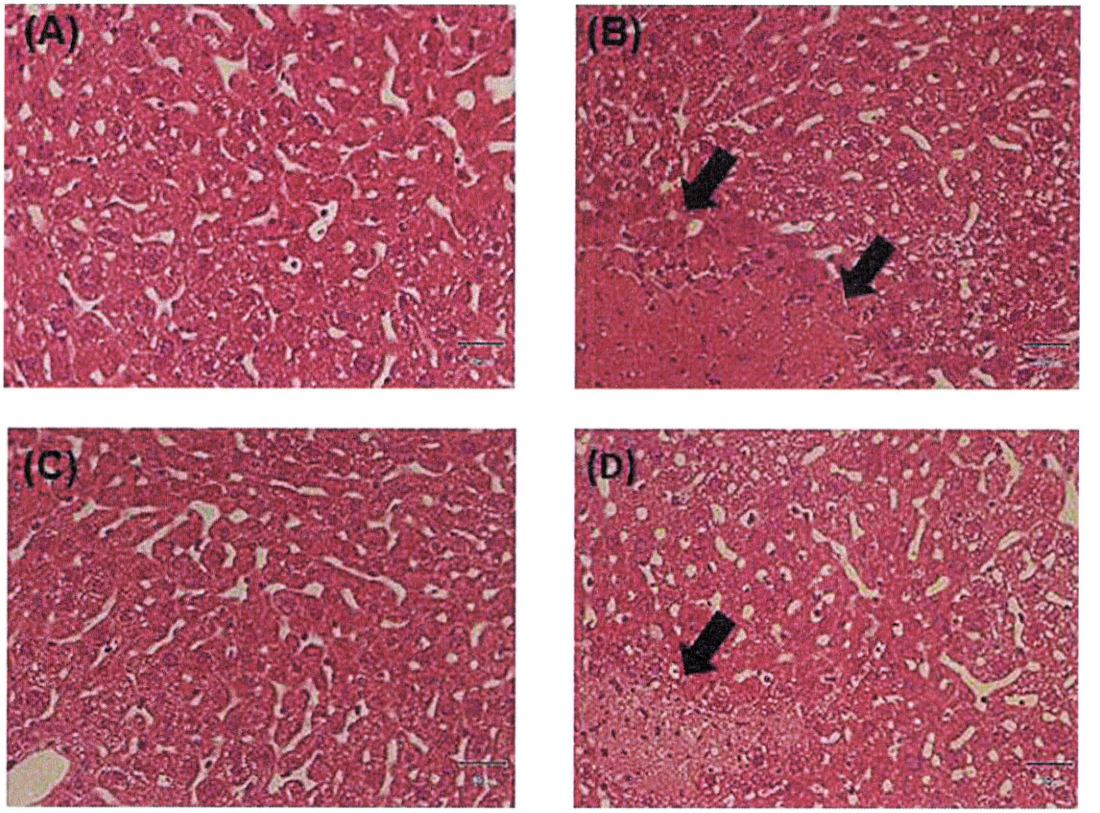

Fig. 2: Hematoxylin and eosin staining of the liver sections. Twenty-four h after administration, the liver was excised from the mice treated with vehicle (A), SP70 (B), SP70-N (C) or SP70-C (D) and fixed with 4% paraformaldehyde. Tissue sections were stained with hematoxylin and eosin and observed under a microscope. The arrows indicate areas of hepatic injury.

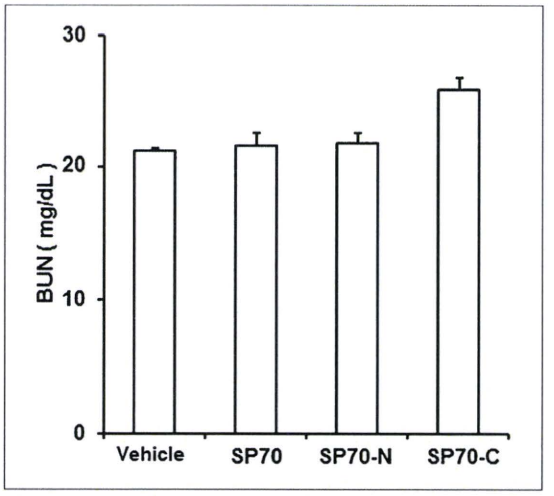

Fig. 3: Effect of SP70-N and SP70-C on kidney. SP70, SP70-N and SP70-C were intravenously administered at 40 mg/kg, 60 mg/kg, and 60 mg/kg, respectively. At 24 h after administration, blood was collected, and the resultant serum was used for the BUN assay with a commercially available kit. Data are means ± SEM (n = 4).

3.3. Biochemical analysis

Serum alanine aminotransferase (ALT) and blood urea nitrogen (BUN) were measured with commercially available kits according to the manufacturer's protocols (Wako Pure Chemical Industries, Osaka, Japan).

3.4. Histological analysis

The liver was excised and fixed with 4% paraformaldehyde. After sectioning, thin tissue sections of tissues were stained with hematoxylin and eosin for histological observation. Liver sections were stained with Azan-Mallory for observation of liver fibrosis.

3.5. Measurement of hydroxyproline content

Hepatic hydroxyproline (HYP) content was measured using Kivirikko's method (Kivirikko et al. 1967), with some modifications. Briefly, liver tissue (50 mg) was hydrolyzed in 6 mol/L HCl at 110 °C for 24 h in a glass test tube. After centrifugation at 3000 rpm for 10 min, 2 mL of the supernatant was neutralized with 8 N KOH. Two grams of KCl and 1 mL of 0.5 mol/L borate buffer were then added to the resultant solution, followed by incubation for 15 min at room temperature and a further incubation for 15 min at 0 °C. Freshly prepared chloramine-T solution was then added and the solution was incubated at 0 °C for 1 h, followed by the addition of 2 mL of 3.6 mol/L sodium thiosulfate. The samples were incubated at 120 °C for 30 min, and then 3 mL toluene was added with incubation for a further 20 min at room temperature. After centrifugation at 2000 rpm for 5 min, 2 mL of the supernatant was added to 0.8 mL of buffer containing Ehrlich's reagent and incubated for 30 min at room temperature. The samples were then transferred to a plastic tube and the absorbance was measured at 560 nm. Hydroxyproline content was expressed as micrograms of hydroxyproline per gram of liver.

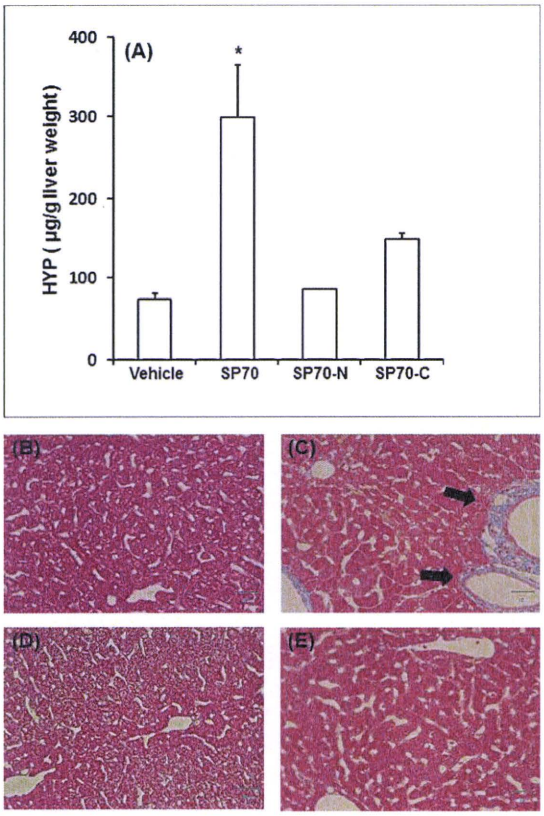

Fig. 4: Effect of SP70-N and SP70-C on chronic liver injury. SP70 was injected into mice every 3 days for 4 weeks at 30 mg/kg. SP70-C and SP70-N was injected into mice every 3 days for 4 weeks at 60 mg/kg. Three days after the last injection, the mice were sacrificed. Hydroxyproline levels (A) in the liver were measured. The liver was excised from mice treated with vehicle (B), SP70 (C), SP70-N (D) or SP70-C (E) and fixed with 4% paraformaldehyde. Tissue sections were stained with Azan and observed under a microscope. The arrows indicate areas of hepatic fibrosis. Data are means ± SEM (n = 4). *$p < 0.05$ as compared to the vehicle-treated group.

3.6. Statistical analysis

The data were analyzed for statistical significance using Dunnett's test. P values less than 0.05 were considered statistically significant.

References

Dobson J (2006) Magnetic micro- and nano-particle-based targeting for drug and gene delivery. Nanomed 1: 31–37.

Kim JS, Yoon TJ, Yu KN, Kim BG., Park SJ, Kim HW, Lee KH, Park SB, Lee JK, Cho MH (2006) Toxicity and tissue distribution of magnetic nanoparticles in mice. Toxicol Sci 89: 338–347.

Kivirikko KI, Laitinen O, Prockop DJ (1967) Modifications of a specific assay for hydroxyproline in urine. Anal Biochem 19: 249–255.

Lin YH, Mi FL, Chen CT, Chang WC, Peng SF, Liang HF, Sung HW (2007) Preparation and characterization of nanoparticles shelled with chitosan for oral insulin delivery. Biomacromolecules 8: 146–152.

Nishimori H, Kondoh M, Isoda K, Tsunoda S, Tsutsumi Y, Yagi K (2009a) Silica nanoparticles as hepatotoxicants. Eur J Pharm Biopharm 72: 496–501.

Nishimori H, Kondoh M, Isoda K, Tsunoda S, Tsutsumi Y, Yagi K (2009b) Histological analysis of 70-nm silica particles-induced chronic toxicity in mice. Eur J Pharm Biopharm 72: 626–629.

Oku N, Tokudome Y, Namba Y, Saito N, Endo M, Hasegawa Y, Kawai M, Tsukada H, Okada, S (1996) Effect of serum protein binding on real-time trafficking of liposomes with different charges analyzed by positron emission tomography. Biochim Biophys Acta 1280: 149–154.

Schiestel T, Brunner H, Tovar G.E (2004) Controlled surface functionalization of silica nanospheres by covalent conjugation reactions and preparation of high density streptavidin nanoparticles. J Nanosci Nanotechnol 4: 504–511.

Smith B, Wepasnick K, Schrote KE, Cho HH, Ball WP, Fairbrother DH (2009) Influence of surface oxides on the colloidal stability of multi-walled carbon nanotubes: a structure-property relationship. Langmuir 25: 9767–9776.

Warheit DB, Sayes CM, Reed KL, Swain KA (2008) Health effects related to nanoparticle exposures: environmental, health and safety considerations for assessing hazards and risks. Pharmacol Ther 120: 35–42.